

LMAPR2451

Atomistic and nanoscopic simulations

Study of FeS₂ and its optical properties

Professors Jean-Christophe Charlier, Xavier Gonze & Gian-Marco Rignanese

Mentors : Alexandre Cloots & Ionel-Bogdan Guster

Anatole Moureaux | 54731700

This report aims to investigate the optical properties of FeS₂. To do so, *ab initio* computations are first performed on a 6-atoms orthorhombic unit cell. The convergence with respect to several structural parameters is also studied. The optical properties are then analyzed in the light of the obtained results. Finally, a comparison is made with the published research, and a discussion about the quality of the simulation is made.

2020-2021

Contents

1	Introduction	2
1.1	Motivation	2
1.2	Pyrite : Overview and Abinit representation	3
2	Convergence studies and pseudopotentials	5
2.1	Additional parameters	5
2.2	Determination of the optimal k -points grid	6
2.3	Convergence of the total energy per atom with respect to the cut-off energy (ecut)	6
2.4	Convergence of the total energy per atom with respect to the number of k -points (ngkpt)	6
2.5	Convergence of acell with respect to the cut-off energy	7
2.6	Convergence of acell with respect to the number of k -points	7
2.7	Summary	7
3	Optical properties	9
3.1	Electronic band structure	9
4	Comparison with the litterature	10
5	Conclusion	11
A	Determination of the optimal k-points grid	13
B	Convergence study with respect to ecut	14
C	Convergence study with respect to ngkpt	15

1 Introduction

1.1 Motivation

Pyrite (FeS_2) is an interesting semiconducting material. Indeed, it can be used in numerous domains, from mechanical applications, where it is appreciated for its toughness and abrasiveness, to optical applications, where it can be used as an high-energy light absorber [1]. As pyrite is very abundant, it can become a material of choice in the industry if correct and valuable uses of the latter could be elaborated. It is depicted on Figure 2.

One of the promising potential application of pyrite is its integration into solar panels. Indeed, pyrite thin films could be good alternatives to the conventional silicon based solar cells, since the latter are more economically and ecologically costly. However, the performances of the material must be similar to or better than materials already used for solar cells, in order to make it truly competitive [2]. It is thus important to assess the different optical characteristics that pyrite is able to present.

Solar cells are a concept that dates all the way back to 1883 [9]. However, it might be interesting to recall some of the main features of those devices. It consists of photoelectric components able to convert the energy of the (solar) light into electricity through the *photovoltaic effect*. More precisely, a solar cell is composed of a *pn*-junction diode, usually made of silicon. When the depletion region of the junction is hit by solar photons, an electron is delivered in the *n*-layer and a hole is delivered in the *p*-layer (Figure 1). By doing so on a large scale, the *pn*-junction is able to generate a voltage of about 0.5 V, if the *n*-doped layer is sufficiently thin (to make the photons reach the depletion region as easily as possible). A solar panel is composed of several solar cells in series, in order to add up the voltage generated by each cell. The best materials for solar cells-related applications are the materials showing :

- a semiconducting behavior
- a high optical absorption coefficient
- a high electrical conductivity
- an abundant presence in the Earth's crust.[3]

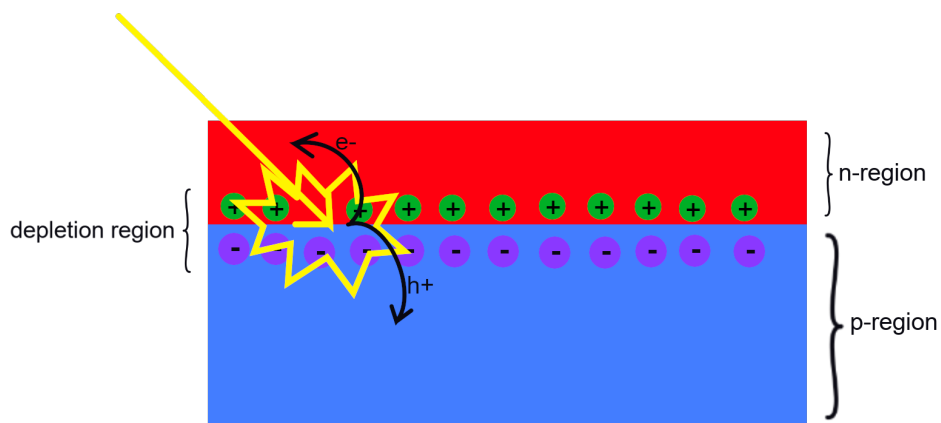


Figure 1: Simplified view of the photovoltaic effect. When a photon hits an atom in the depletion region, an electron is released in the *n*-region and a hole is released in the *p*-region, creating a voltage when done multiple times.

Even if bulk pyrite shows a *n*-type behavior, pyrite thin-films show a *p*-type behavior. Only the deposition of a thin layer of *n*-type semiconductor on the pyrite film is needed to form a *pn*-heterojunction. Furthermore, the pyrite has a strong absorption coefficient. It thus allows to decrease the thickness of the pyrite film, which is helpful to improve the performances of the *pn*-junction, and hence, of the solar cell [4]. Plus, it is abundant in the soil. Pyrite thus seems to be a material of choice for solar cells-related applications.

However, serious limitations prevent pyrite to be highly performant in solar cells-based applications. Indeed, a very poor solar energy conversion efficiency is observed when assessing the performances of pyrite solar cells. That low efficiency is presumably due to a low photovoltage generation. The sources of that low photovoltage is highly debated among the scientific community. Several sources have been proposed over the years : detrimental S vacancies (although stoichiometric pyrite shows the same low photovoltage), detrimental impurities or even lattice defects [5]. No consensus has been found nowadays. But as pyrite could be a game-changer in the solar cell industry if its efficiency was improved, it is worth to look a little closer to the optical properties of the material.

In the following report, the properties of the PNNM FeS₂ will be studied using the **Abinit** package. First, the unit cell and its structural parameters will be described, based on the Materials Project documentation¹. Then, the representation of the crystal in **Abinit** will be presented (thus describing the main parameters of the `.abi` files to be used). Secondly, the pseudopotential and the approximation used in the first place will be discussed. Then, convergence studies based on the energy cut-off (`ecut`) and the number of *k*-points (`ngkpt`) will be performed. When a proper (`ecut,ngkpt`) will have been determined, a discussion about the pseudopotential and the approximation will be held, and possible alternatives will be presented. Finally, additional **Abinit** computations will be made, and the optical properties will be studied through other characteristics of the material. To conclude, the performances of pyrite in solar cells-based applications will be discussed.

1.2 Pyrite : Overview and Abinit representation

The pyrite (FeS₂) primitive cell contains 2 Fe atoms and 4 S atoms, and is part of the orthorhombic system (Figure 3). The space group is PNNM[58] in the Hermann-Mauguin notation.

Furthermore, it is a semiconductor. The energy of the indirect bandgap $((0 \ 0.4 \ 0) - U)$ is about 0.978 [eV][6].

Finally, the primitive cell will be represented as follow in **Abinit** input files :

```
acell  3.390 4.438 5.411 Angstr # the lattice vectors scaling
ntypat 2                        # there are two types of atoms in the
                                # primitive cell : Fe and S
znuc1  26 16                  # Fe has 26 electrons and S has 16
natom  6                      # there are 6 atoms in the primitive cell
typat   1 1 2 2 2 2          # 2 Fe atoms and 4 S atoms
xred    0      0      0      # position of the first Fe atom in reduced coordinates
        0.5    0.5    0.5    # position of the second Fe atom
        0      0.206  0.3753  # position of the first S atom
        0      0.794  0.6247  # position of the second S atom
        0.5    0.294  0.8753  # position of the third S atom
        0.5    0.706  0.1247  # position of the fourth S atom
```

¹<https://materialsproject.org/materials/mp-1522/>

The data also comes from [6].



Figure 2: Extracted form (ore) of pyrite.
"Pierre Pyrite", France Minéraux, 2021.

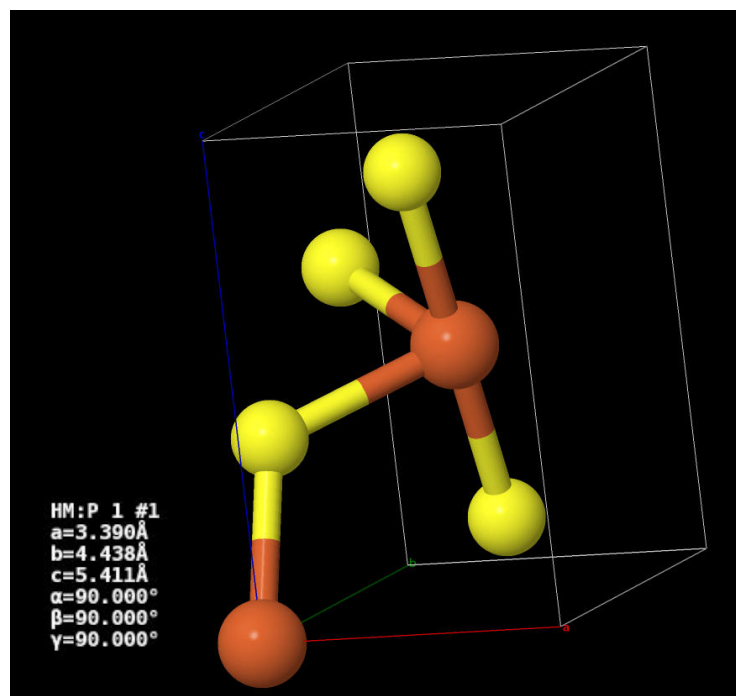


Figure 3: Primitive cell of FeS_2 .
Materials Project (mp-1522), Jmol

2 Convergence studies and pseudopotentials

In **Abinit** computations, convergence studies are very important, as it help to make sure that some of the chosen parameters, like the cut-off energy (**ecut**) or the number of k -points in the cell (determined by the sampling of the Brillouin zone **ngkpt**), allow the most accurate results as possible. To do such analysis, the same computations are done with a dataset concerning the parameter of interest, with an increasing accuracy of the environment. The evolution of some resulting variables, like the total energy of the unit cell (**etotal**), indicates when the parameters of interest allow a sufficiently accurate simulation.

In the following subsections, the convergence studies with respect to **ecut** and **ngkpt** will be performed. One could also choose to study the convergence of the simulation with respect to the scaling of the lattice parameters (**acell**). However, the complexity of this kind of study increases pretty fast with the number of atoms in the unit cell, and as pretty accurate values were found on the Materials Project, this study won't be performed here. It is still possible to optimize the shape and the volume of the unit cell when the final **ecut** and **ngkpt** are chosen, in order to get the most accurate future computations as possible.

2.1 Additional parameters

To begin, we will use the *Local spin Density Approximation* (LDA) functional. Indeed, it is widely used and works well in many simulations. The pseudopotentials that will be used are retrieved from the pseudodojo [8]. Two pseudopotentials are used : the NC SR (ONCVSPSP v0.4.1) LDA standard pseudopotential relative to Fe, and the same one but relative to S (both in psp8 format). The pseudopotentials respectively

It is also important to properly define the parameters ruling the SCF procedure. The most important one is **nstep**, defining the number of SCF cycles. It is set to 100 in the first place. **toldfe** is set to 1.0d-10 Ha, ensuring a pretty accurate convergence with respect to the total energy. **toldfe** is chosen as the structural relaxation is not performed yet (in that case, **toldff** is preferably used). Although it is not mandatory, the SCF procedure can be preconditioned by specifying the macroscopic dielectric constant (**diemac**). It is used to speed up the SCF procedure. A value of 24 is chosen, accordingly to [6].

Finally, the parameters of the k -points grid must be specified. **kptopt** is set to 1 in order to take advantage of the symmetry of the unit cell. By setting **prtkpt** to 1, **Abinit** will generate a set of k -point grids, that will be helpful to optimize further computations and convergence studies.

```
pseudos "pdj_nc_sr_041_lda_standard_psp8/Fe.psp8, pdj_nc_sr_041_lda_standard_psp8/S.psp8"

# parameters of the SCF procedure :
nstep      100      # maximal number of SCF cycles
toldfe     1.0d-10  # SCF procedure will stop when the difference of total energy
                  # between two iterations will be lower than toldfe Hartree
diemac     24.0     # preconditioning of the SCF procedure.

# parameters of the k-points grid :
kptopt     1
prtkpt     1
```

2.2 Determination of the optimal k -points grid

The first simulation will be used to generate k -points grids and the corresponding shifts (`shiftk`). `Abinit` was run with the input file `1522_1_kpointsgrids.abi` (Appendix A), performing the analysis of a series of 70 different k -grids. The lists were provided with the corresponding `kptrlatt`, `shiftk`, `kpstrlen` and `nkpt` parameters. An additional list containing the best k -grids was also provided, helping to have a better idea of the k -points distribution in the irreducible Brillouin zone.

To conclude, the default Monkhorst-Pack grids will be used, by using

```
ngkpt    4 4 4
nshiftk   1
shiftk    0.5 0.5 0.5
```

2.3 Convergence of the total energy per atom with respect to the cut-off energy (`ecut`)

The study of the convergence of the simulation was performed by running `Abinit` with the input file `1522_2_ecutConv.abi` (Appendix B). The total energy per atom of the unit cell is then plotted versus `ecut` (which spans from 10 [Ha] to 58.33 [Ha]) (Figure 4). Upper and lower bounds of ± 0.5 [mHa] are set around the last obtained value. It allows to determine the first `ecut` for which the convergence is reasonable. In the present case, `ecut` = 40 [Ha].

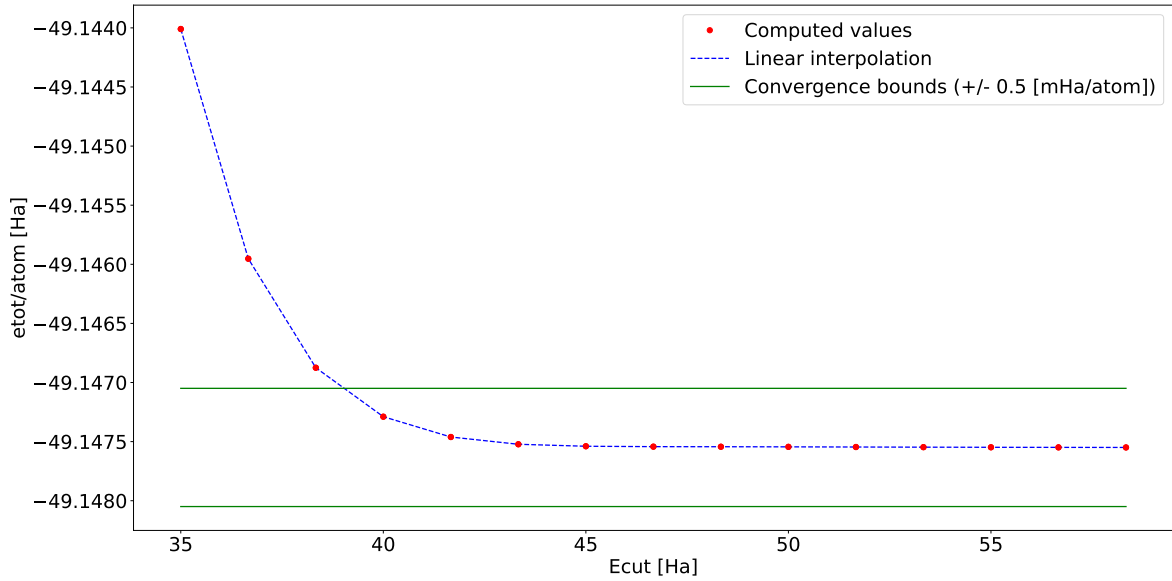


Figure 4: Total energy per atom with respect to the cut-off energy. Linear interpolations are for visual guidance only.

2.4 Convergence of the total energy per atom with respect to the number of k -points (`ngkpt`)

Alternatively, the same kind of study is done for the number of k -points in the lattice. `Abinit` is run with the input file `1522_2_nkpConv.abi` (Appendix C). The energy per atom can be plotted versus the `ngkpt` parameter (Figure 5).

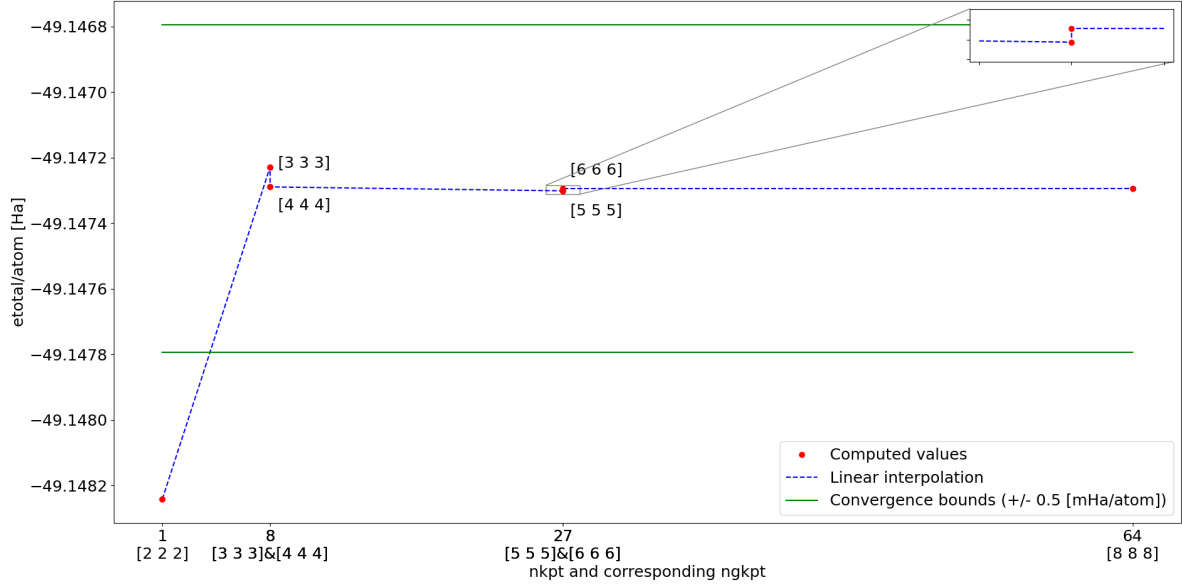


Figure 5: Total energy per atom with respect to the number of k -points in the k -points grid. Linear interpolations are for visual guidance only.

The first converged **ngkpt** value is [3 3 3].

Concerning the convergence of the total energy per atom, the couple of values (**ecut**,**ngkpt**) that will be used in the further computations is thus (40 [Ha], [3 3 3]).

2.5 Convergence of **acell** with respect to the cut-off energy

The convergence of the length scales of the unit cell was performed using a dataset of **ecut** values between 20 [Ha] and 50 [Ha], **ngkpt** = [4 4 4] and **ecutsm** = 0.5 [Ha]. The results are displayed on Figure 6. The first converged value is 30 [Ha].

2.6 Convergence of **acell** with respect to the number of k -points

The convergence of the length scales of the unit cell was analyzed with **ecut** = 40 [Ha] and **ecutsm** = 0.5 [Ha]. The results are displayed on Figure 7. It can be seen that [2 2 2] is already in the limits of 0.2% of the length. Therefore, the value [2 2 2] is considered as the first converged value.

2.7 Summary

	ecut [Ha]	ngkpt
Convergence of etotal/atom	40	[3 3 3]
Convergence of acell	30	[2 2 2]

Furthermore, the most accurate value for **acell** and **xred**, obtained with **ngkpt** = [8 8 8] (**nkpt** = 64) and **ecut** = 40 [Ha], is

acell (1)	6.2637308171 Bohr
acell (2)	8.2001290166 Bohr
acell (3)	9.9979491007 Bohr

or

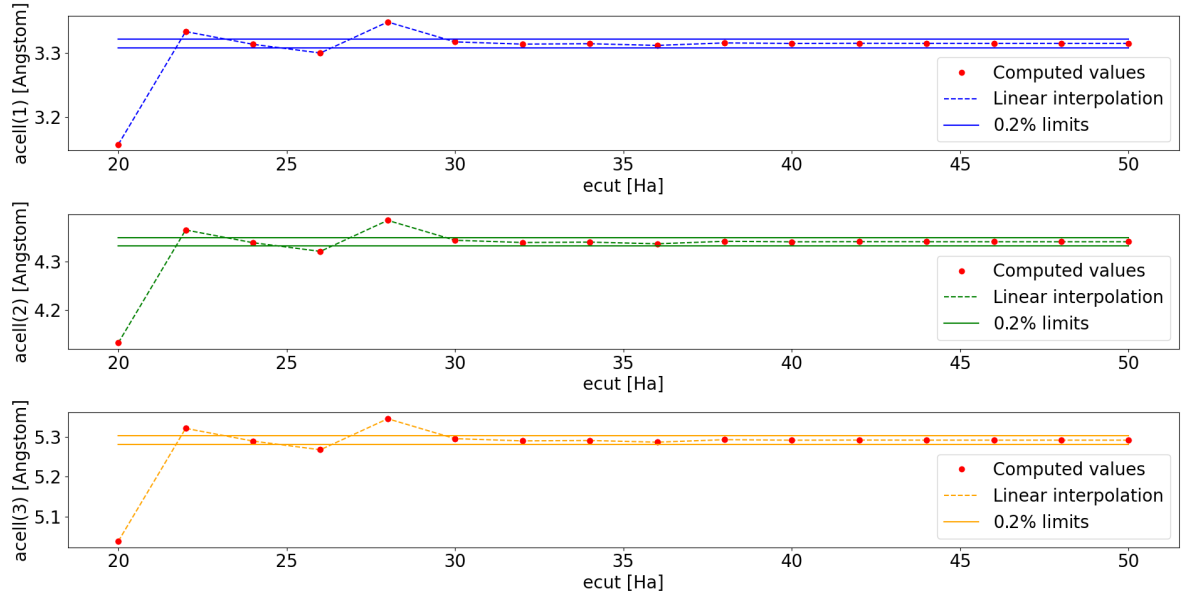


Figure 6: Convergence of the length scales acell with respect to the cut-off energy ecut .

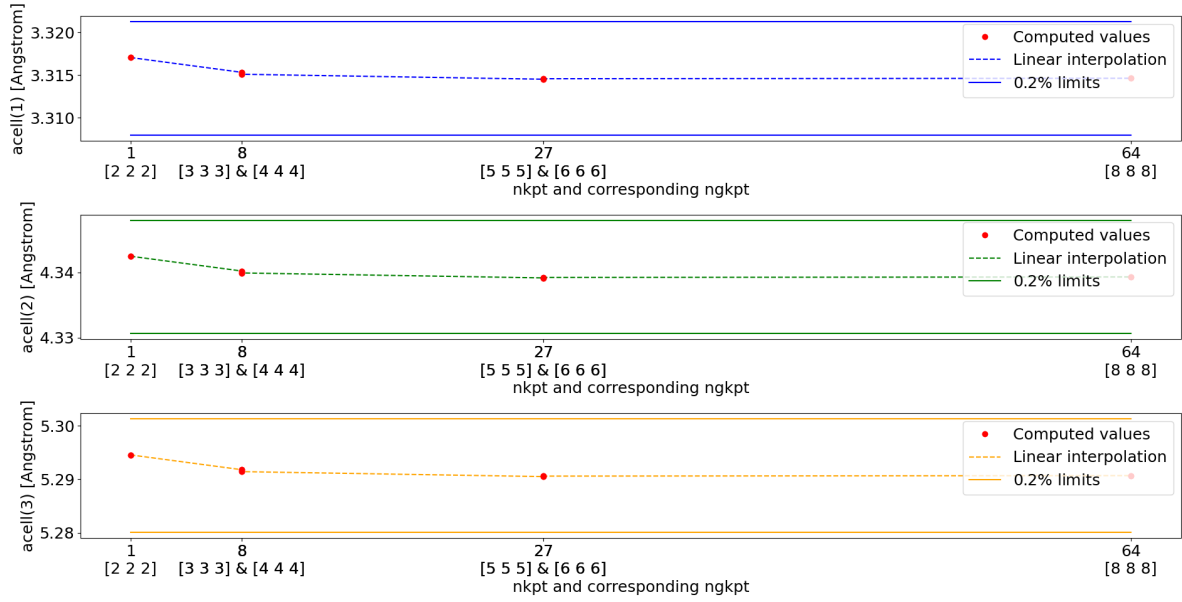


Figure 7: Convergence of the length scales acell with respect to the number of k -points in the k -points grid.

acell(1)	3.31462360299498 Angstroms
acell(2)	4.33932140120453 Angstroms
acell(3)	5.29068681882879 Angstroms

and

	xred(1)	xred(2)	xred(3)
Fe #1	0.0000000000	-8.2954404041E-21	3.7707082665E-20
Fe #2	5.0000000000E-01	5.0000000000E-01	5.0000000000E-01
S #1	0.0000000000E+00	2.0805564362E-01	3.7373683165E-01
S #2	0.0000000000E+00	7.9194435638E-01	6.2626316835E-01
S #3	5.0000000000E-01	2.9194435638E-01	8.7373683165E-01
S #4	5.0000000000E-01	7.0805564362E-01	1.2626316835E-01

3 Optical properties

3.1 Electronic band structure

The band structure of the material was computed as follows. First, an optimal k -path was obtained using Abipy. Then, 50 bands were analyzed using the parameters from the previous convergence studies (`ecut` = 30 Ha and `ngkpt` = [2 2 2]). A self-consistent density computation was done beforehand. The band structure is represented on ???. From the data, the Fermi energy was found to be 9.03565 eV and the band gap 0.735835 eV. \\TODO

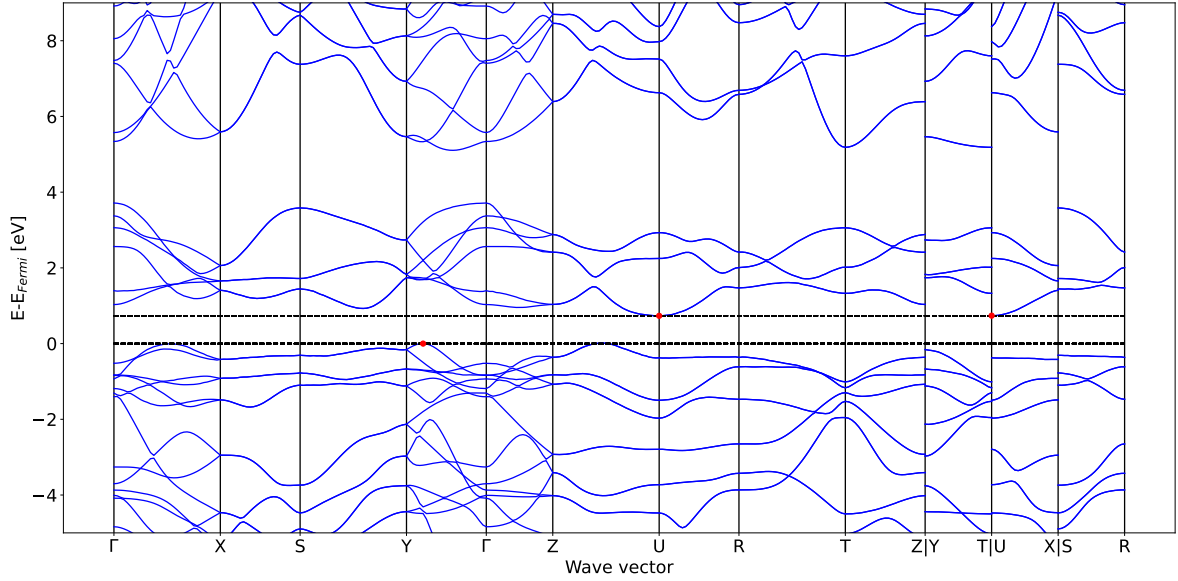


Figure 8: Band structure of FeS₂. The red dots represent the valence band minimums and the conduction band maximum.

- Compute the electronic band structure
- compute the phonon dispersion
- Implications for a thin film used in a solar cell

4 Comparison with the literature

\\TODO

- Compare with the material project + other sources if needed
- Discuss the differences and the similitudes

5 Conclusion

\\TODO

- Summary of the study - What has been learned ?
- What implications in real life applications ?
- What further studies could be done ?

References

- [1] "Pyrite de fer - Utilisations et applications | African Pegmatite", African Pegmatite, 2021. [Online]. Available: <https://mineralmilling.com/fr/pyrite-de-fer-utilisations-et-applications/>. [Accessed: 04- Apr- 2021].
- [2] M. Hutchins, "A long way to go for iron pyrite solar cells", pv magazine International, 2021. [Online]. Available: <https://www.pv-magazine.com/2020/06/15/a-long-way-to-go-for-iron-pyrite-solar-cells/>. [Accessed: 04- Apr- 2021].
- [3] "Solar Cell: Working Principle & Construction (Diagrams Included)", Electrical4U, 2021. [Online]. Available: <https://www.electrical4u.com/solar-cell/>. [Accessed: 05- Apr- 2021].
- [4] M. Limpinsel, "Iron Pyrite Absorbers for Solar Photovoltaic Energy Conversion", University of California, 2015. Available: <https://escholarship.org/uc/item/8042w4kd>. [Accessed 5 April 2021].
- [5] M. Rahman and T. Edvinsson, "What Is Limiting Pyrite Solar Cell Performance?", Joule, vol. 3, no. 10, pp. 2290-2293, 2019. Available: 10.1016/j.joule.2019.06.015.
- [6] "mp-1522: FeS2 (orthorhombic, Pnnm, 58)", Materialsproject.org, 2021. [Online]. Available: <https://materialsproject.org/materials/mp-1522/>. [Accessed: 06- Apr- 2021].
- [7] "Pierre Pyrite", France Minéraux, 2021. [Online]. Available: <https://www.france-mineraux.fr/vertus-des-pierres/pierre-pyrite/>. [Accessed: 07- Apr- 2021].
- [8] D. Hamann, "Optimized norm-conserving Vanderbilt pseudopotentials", 2021.
- [9] "Cellule photovoltaïque — Wikipédia", Fr.wikipedia.org, 2021. [Online]. Available: https://fr.wikipedia.org/wiki/Cellule_photovolt%C3%AFque#Histoire. [Accessed: 07-May-2021].

A Determination of the optimal k -points grid

Name of the input file : 1522_1_kpointsgrids.abi

```
acell      3.390 4.438 5.411 Angstr # the lattice vectors scaling
ntypat     2                        # there are two types of atoms in the
                                           # primitive cell : Fe and S
znucl      26 16                    # Fe has 26 electrons and S has 16
natom       6                      # there are 6 atoms in the primitive cell
typat      1 1 2 2 2 2              # 2 Fe atoms and 4 S atoms
xred        0      0      0         # position of the first Fe atom in reduced coordinates
                                           # position of the second Fe atom
0.5      0.5      0.5
0      0.206  0.3753                # position of the first S atom
0      0.794  0.6247                # position of the second S atom
0.5      0.294  0.8753                # position of the third S atom
0.5      0.706  0.1247                # position of the fourth S atom

pseudos    "Fe.psp8,S.psp8"

# parameters of the SCF procedure :
nstep      50                      # maximal number of SCF cycles
toldfe     1.0d-10                  # SCF procedure will stop when the difference of total
                                           # energy between two iterations will be lower than
                                           # toldfe Hartree
diemac     24.0                    # preconditioning of the SCF procedure.

# parameters for generating the k-points grids :
kptopt     1
prtkpt     1
```

B Convergence study with respect to ecut

Name of the input file : 1522_2_ecutConv.abi

```
acell      3.390 4.438 5.411 Angstr
ntypat     2
znuc1      26 16
natom      6
typat      1 1 2 2 2 2
xred       0      0      0
           0.5    0.5    0.5
           0      0.206  0.3753
           0      0.794  0.6247
           0.5    0.294  0.8753
           0.5    0.706  0.1247
```

```
pseudos    "Fe.psp8,S.psp8"
```

```
# parameters of the SCF procedure :
```

```
nstep      100                      # maximal number of SCF cycles
toldfe     1.0d-10                  # SCF procedure will stop when the difference of total
                                     # energy between two iterations will be lower than
                                     # toldfe Hartree
diemac     24.0                     # preconditioning of the SCF procedure.
```

```
# parameters for generating the k-points grids :
```

```
kptopt     1
ngkpt      4 4 4
nshiftk    1
shiftk     0.5 0.5 0.5
```

```
ndtset     30
ecut:      10
ecut+      4/3
```

C Convergence study with respect to ngkpt

Name of the input file : 1522_2_nkpConv.abi

```
acell      3.390 4.438 5.411 Angstr
ntypat     2
znucl      26 16
natom       6
typat      1 1 2 2 2 2
xred        0      0      0
            0.5    0.5    0.5
            0      0.206  0.3753
            0      0.794  0.6247
            0.5    0.294  0.8753
            0.5    0.706  0.1247
ecut       40                                # the converged value for ecut

pseudos    "/Fe.psp8,S.psp8"

# parameters of the SCF procedure :
nstep      100                                # maximal number of SCF cycles
toldfe     1.0d-10                            # SCF procedure will stop when the difference of total
                                                # energy between two iterations will be lower than
                                                # toldfe Hartree
diemac     24.0                              # preconditioning of the SCF procedure.

# parameters for generating the k-points grids :
getwfk     -1
kptopt      1
ndtset      6
ngkpt1     2 2 2
ngkpt2     3 3 3
ngkpt4     5 5 5
ngkpt5     6 6 6
ngkpt6     8 8 8
nshiftk     1
shiftk      0.5 0.5 0.5
```